

PHYSICAL REVIEW E

STATISTICAL PHYSICS, PLASMAS, FLUIDS, AND RELATED INTERDISCIPLINARY TOPICS

THIRD SERIES, VOLUME 61, NUMBER 4 PART A

APRIL 2000

RAPID COMMUNICATIONS

The Rapid Communications section is intended for the accelerated publication of important new results. Since manuscripts submitted to this section are given priority treatment both in the editorial office and in production, authors should explain in their submittal letter why the work justifies this special handling. A Rapid Communication should be no longer than 4 printed pages and must be accompanied by an abstract. Page proofs are sent to authors.

Multifractal properties of the random resistor network

M. Barthélémy,^{1,*} S. V. Buldyrev,¹ S. Havlin,² and H. E. Stanley¹

¹Center for Polymer Studies and Department of Physics, Boston University, Boston, Massachusetts 02215

²Minerva Center and Department of Physics, Bar-Ilan University, Ramat-Gan 52900, Israel

(Received 25 August 1999)

We study the multifractal spectrum of the current in the two-dimensional random resistor network at the percolation threshold. We consider two ways of applying the voltage difference: (i) two parallel bars, and (ii) two points. Our numerical results suggest that in the infinite system limit, the probability distribution behaves for small i as $P(i) \sim 1/i$, where i is the current. As a consequence, the moments of i of order $q \leq q_c = 0$ do not exist and all currents of value below the most probable one have the fractal dimension of the backbone. The backbone can thus be described in terms of only (i) blobs of fractal dimension d_B and (ii) high current carrying bonds of fractal dimension going from $1/\nu$ to d_B .

PACS number(s): 64.60.Ak, 05.45.Df

The transport properties of the percolating cluster have been the subject of numerous studies [1,2]. A particularly interesting system is the random resistor network (RRN), where the bonds have a random conductance. The random resistor network serves as a paradigm for many transport properties in heterogeneous systems as well as being a simplified model for fracture [3].

The first studies of the RRN were devoted to effective properties of the network (conductivity, permittivity, etc.) [4,5], but for many practical applications, such as fracture, and dielectric breakdown [3], the central quantity is the probability distribution $P(i)$ of currents i . For instance, in the random fuse network, it is the maximum current corresponding to the hottest or “red” bonds which will determine the macroscopic failure of the system [3].

The probability distribution $P(i)$ has many interesting features, one of which is multifractality [6–13]: in order to describe $P(i)$, an infinite set of exponents is needed. This idea of multifractality was initially proposed to treat turbulence [14] and later applied successfully in many different

fields, ranging from model systems such as DLA [15] to physiological data such as heartbeat [16].

It was first believed [8,9] that the low current part of $P(i)$ and of the multifractal spectrum follow a log-normal law as it is the case on hierarchical lattices. It is now clear [17,18] that for small currents, the current probability distribution follows a power law $P(i) \sim i^{b-1}$, where $b \geq 0$. For large currents, there is a weak dependence on the system size L . This is in contrast with small currents, which are governed by very long paths, and therefore depend more strongly on L . It was suggested [17,18] that the exponent b of the low-current part has a $1/\log L$ dependence, where L is the system size. The asymptotic value b_∞ of the exponent b is of crucial importance. If b_∞ is finite and positive, then a low current evolves on a subset with a fractal dimension depending on its value. On the other hand, if b_∞ is zero, then the low current part of the multifractal spectrum is flat and the entire backbone is contributing to low currents. It is thus important to understand if the apparent subset structure with different fractal dimensions is a finite-size effect.

This problem was addressed by Batrouni *et al.* [17] who conjectured a zero asymptotic slope, and by Aharony *et al.* [18] who proposed a finite asymptotic value. The maximum value of L in the literature is 128 [17], so numerical esti-

*Permanent address: CEA-BIII, Service de Physique de la Matière Condensée, 91680, Bruyères-Le-Châtel, France.

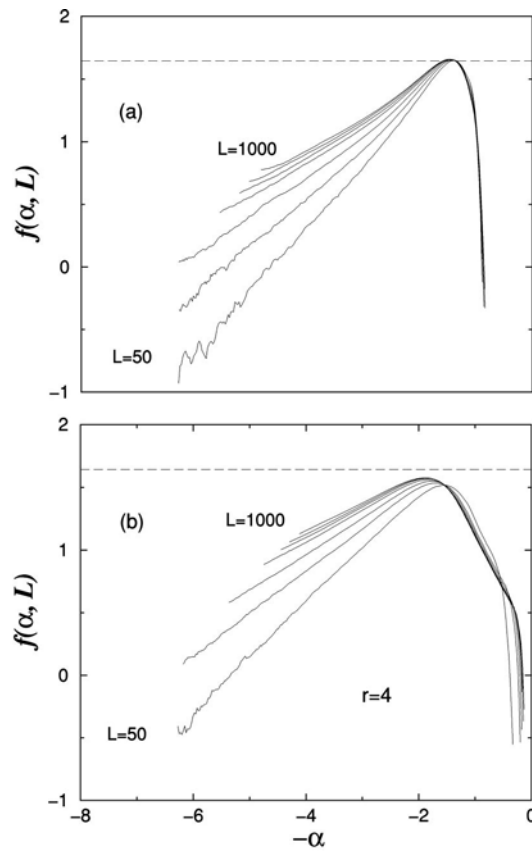


FIG. 1. Multifractal spectra for fixed voltage for (a) parallel bars and (b) for two injection points separated by a distance $r=4$. We show the results for seven different values of $L=50,100,200,400,600,750,1000$ and averaged over 10^4 configurations (L increases from the bottom to the top). The horizontal dashed line is at $d_B \approx 1.643$.

mates could not lead to a definite conclusion. In this Rapid Communication, we present evidence that the asymptotic slope is zero.

We first recall the basis of multifractality applied to the percolating two-dimensional resistor network of linear size L . Let $n(i, L)$ be the number of bonds carrying current i . By the steepest descent method, the main contribution to $n(i, L)$ for large L is given by [8,9]

$$n(i, L) \sim L^{f(\alpha, L)}, \quad (1)$$

where $\alpha \equiv -\log i/\log L$. The multifractal spectrum $f(\alpha, L) \equiv \log n/\log L$ can thus be interpreted as the fractal dimension of the subset of bonds carrying the current i . The q th moment of the current is defined as $M_q \equiv \langle \sum i^q \rangle$, where the sum is over all bonds carrying a nonzero current and $\langle \cdot \rangle$ denotes an average over different disorder configurations. These moments exist for $q > q_c$, and it can be easily shown [18] that the “threshold” is $q_c = -b$. The asymptotic slope thus give the asymptotic value of the threshold q_c .

For the fixed current ensemble, one observes that [8,9] $M_q \sim L^{\tau_q}$ for large L and for $q > q_c$ and where τ_q is a universal exponent. In particular, $\tau_0 = d_B$, $\tau_2 = t/\nu$, and $\tau_\infty = 1/\nu$ [19], where d_B is the fractal dimension of the backbone, t the conductivity exponent, and ν is the correlation length exponent. If the behavior is monofractal, then τ_q is a linear func-

tion of q , while in the multifractal case, the exponents are not described by a simple linear function of q . In the $L \rightarrow \infty$ limit, knowing $f(\alpha)$ is equivalent to knowing the infinite set of exponents τ_q , as $f(\alpha)$ is the Legendre transform of τ_q [3].

The low current part of $f(\alpha, L)$ was found numerically to be a power law of slope $b = b(L)$, where [17]

$$b(L) = b_\infty + \frac{A}{\log L} + \varepsilon(L) \quad (2)$$

and $\varepsilon(L)$ is a correction decreasing faster than $1/\log L$ when L is increasing. This equation shows a strong finite-size effect since $\log L$ grows very slowly, and two possibilities for b_∞ were proposed, $b_\infty = 0$ [17] or $b_\infty = 1/4$ [18].

We consider the two-dimensional random resistor network at criticality, i.e., the fraction of conducting bonds p is equal to its critical value $p = p_c = 1/2$. We first apply a voltage difference between two parallel bars. We compute $f(\alpha, L)$, for a fixed voltage difference, for $L = 50, \dots, 1000$, and average over 10^4 configurations for each L . We show our results in Fig. 1(a). The slope is clearly decreasing with L , confirming the strong finite-size effects already observed [17,18].

Next, we consider a second type of configuration, which we call the “two injection points” case, in contrast to the usual “parallel bars” case. We impose a voltage difference between two points P and Q separated by a distance r , and we look for the backbone connecting these two points. This situation was studied in [20,21], but here we keep only the backbones of size L . In this way, we have large backbones connecting the two points P and Q , and for $r \ll L$ we expect to have a large number of small currents on bonds belonging to long loops. The multifractal spectrum is then defined in the same way as for the parallel bars and we calculate for different values of L the slope of its small-current part. The multifractal spectrum in this case is shown in Fig. 1(b). We observe that there is a large amount of small currents, and that the asymptotic limit is reached faster in the two injection points case. We expect that the low current distribution will be asymptotically the same as in the parallel bar case, so the consistency between the two configurations will support our results. However, for large currents there are some distinct differences in the multifractal spectrum [22].

Figure 2(a) shows the slope b versus $1/\log L$ according to Eq. (2) for both multifractal spectra. The extrapolation to $L = \infty$ is consistent with $b_\infty = 0$ in both cases. This result is consistent with the behavior of the successive intercepts [Fig. 2(b)].

Another functional form of b versus L could lead to another value of b_∞ . If we replace the abscissa of Fig. 2(a) by $1/(\log L)^\kappa$, then we find that the extrapolated value for b_∞ depends on κ , ranging from $b_\infty \approx 0.10$ for $\kappa = 2$ to $b_\infty < 0$ (which is impossible) for $\kappa = 0.5$. It is numerically difficult to distinguish between a $1/\log L$ and a $1/(\log L)^2$ behavior, but the $1/\log L$ is the most commonly used [17,18].

In Fig. 2(a), we observe higher order corrections to the behavior $b(L) = b_\infty + A/\log L$. A better fit can be obtained by adding to the linear form a small quadratic term $B/(\log L)^2$ (and eventually even cubic and quartic terms). We find that we cannot do a quadratic fit over the whole range of $1/\log L$, and indeed this leads to two nonphysical results: (a) For both

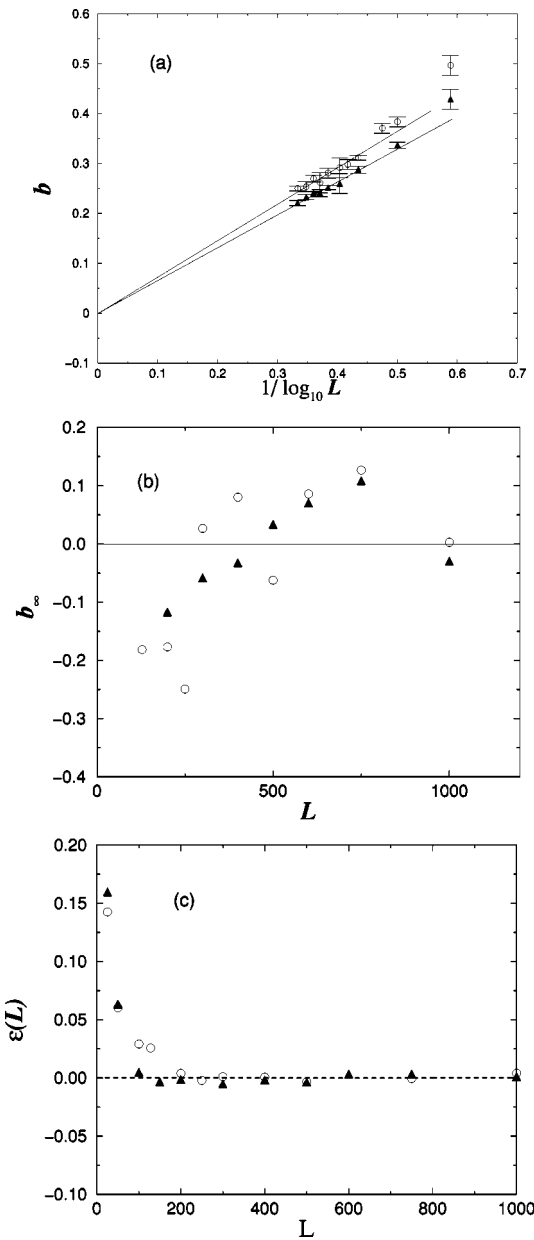


FIG. 2. (a) Slope b vs $1/\log L$. The circles correspond to the parallel bars case and the triangles to the two injection points case. These values were obtained by fitting the small current parts of Figs. 1(a) and 1(b) roughly over the range $2.5 < \alpha < 5$. The extrapolation shown as a guide to the eye is consistent with $b_\infty = 0$. The error bars where estimated by computing the local slopes and are going from 0.02 to 0.005 as L increases. (b) Successive intercepts computed by using a least square fit over three successive points. The circles correspond to the parallel bars case, the triangles to the two injection points case. These plots are consistent with $b_\infty = 0$. (c) Correction $\epsilon(L)$ for $L=25$ to $L=1000$ as given by Eq. (2). This plot shows the fast decay of the correction.

geometries, the fits have *negative* slopes at $1/\log L=0$, which is not physical since the larger the system size, the larger the number of small currents, so the behavior of b should be monotonically decreasing with L . (b) A second defect of these quadratic fits is that the obtained values for the intercepts are *different* for the two geometries, which is impossible.

The important assumption here is the behavior of the

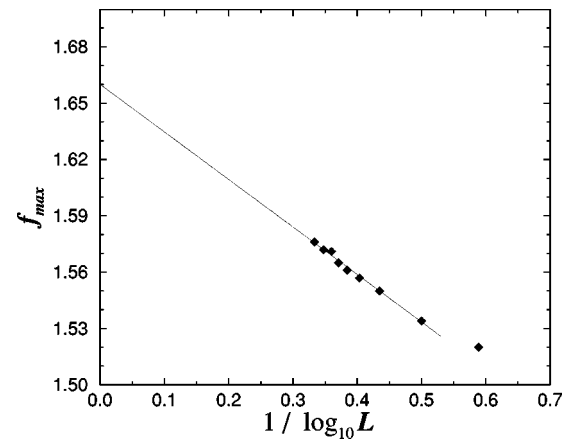


FIG. 3. Maximum of $f(\alpha, L)$, $f_{max}(L)$, in the two injection points case vs $1/\log_{10} L$. The least square fit shown gives the extrapolated value at $L \rightarrow \infty$ of d_B close to the accepted value of 1.64. Also, we found that a log-log plot of $d_B - f_{max}(L)$ vs L is remarkably straight, with slope ≈ -0.20 .

leading term. There is no proof that the leading term of the expansion is $1/\log L$ rather than $(1/\log L)^\kappa$ with $\kappa \neq 1$. However, the assumption that the leading term of the expansion is $1/\log L$ with $b_\infty = 0$ is consistent with our numerical data, and shows that the correction $\epsilon(L)$ decays faster than an inverse power of $\log L$ [see Fig. 2(c)]. Finally, we note that the sequence of maximum values of $f(\alpha, L)$ for the two injection points case plausibly extrapolates in the variable $1/\log L$ as $L \rightarrow \infty$ to a value of d_B close to the known value 1.64 (Fig. 3).

Thus our results suggest the intriguing possibility that for $L \rightarrow \infty$, the small-current part of $f(\alpha, L)$ is a horizontal line at the value d_B , implying that in an infinite system the fractal dimension of the subset contributing to small current is d_B , independent of the value of α . In this sense, the small-current probability distribution is apparently not multifractal. The ‘perfectly balanced’ bonds which carry zero current have a fractal dimension equal to d_B [17]. Since these bonds contribute to $f(\alpha, L)$ for $\alpha \rightarrow \infty$, the fact that their fractal dimension is d_B supports our hypothesis that $b_\infty = 0$. A related conclusion is that $q_c = 0$, or the negative moments of the current do not exist in the infinite-size limit. In particular, it shows that the first-passage time for a tracer particle traveling in a flow field in a porous medium modeled by a percolation cluster diverges in an infinite system.

Moreover, the result $b_\infty = 0$ is supported by the following argument. If b_∞ were not zero, then the number of bonds carrying a small current i would be $n(i \rightarrow 0, L = \infty) \sim i^{b_\infty}$. This behavior would indicate that the number of bonds carrying a small current i approaches zero when $i \rightarrow 0$, which seems unlikely, since on an infinite backbone, the number of loops is very large, and $n(i \rightarrow 0, L = \infty)$ should be nonzero. Hence $b_\infty = 0$. This argument is consistent with the fact that the total number of bonds carrying a nonzero current, $\int_0 n(i, L) d(\log i)$, should diverge as $L \rightarrow \infty$.

For large values of the current, the multifractal features do not change as L increases, suggesting that in the infinite-size limit, there are essentially two different type of subsets. The

first set comprises the blobs of fractal dimension d_B , and the second set comprises links carrying larger values of the current (red bonds), of fractal dimension ranging from $d_{\text{red}} = 1/\nu$ to d_B .

We thank L.A.N. Amaral for valuable help, J.S. Andrade, A. Chessa, A. Coniglio, N.V. Dokholyan, P. Gopikrishnan, P.R. King, G. Paul, A. Scala, and F.W. Starr for useful discussions, and DGA and BP Amoco for financial support.

-
- [1] D. Stauffer and A. Aharony, *Introduction to Percolation Theory* (Taylor and Francis, London, 1992).
 - [2] A. Coniglio and M. Zannetti, Physica D **38**, 37 (1989).
 - [3] *Statistical Models for the Fracture of Disordered Media*, edited by H.J. Herrmann and S. Roux (North-Holland, Amsterdam, 1990).
 - [4] R. Landauer, in *Proceedings of the First Conference on Electrical and Optical Properties of Inhomogeneous Media*, edited by J. C. Garland and D. B. Tanner, AIP Conf. Proc. No. 40 (AIP, New York, 1978).
 - [5] D. J. Bergman and D. Stroud, Solid State Phys. **46**, 147 (1992).
 - [6] L. de Arcangelis, S. Redner, and A. Coniglio, Phys. Rev. B **31**, 4725 (1985); R. Rammal, C. Tannous, and A.-M. S. Tremblay, Phys. Rev. A **31**, 2662 (1985).
 - [7] R. Rammal, C. Tannous, P. Breton, and A.-M. S. Tremblay, Phys. Rev. Lett. **54**, 1718 (1985).
 - [8] L. de Arcangelis, S. Redner, and A. Coniglio, Phys. Rev. B **34**, 4656 (1986).
 - [9] L. de Arcangelis, A. Coniglio, and S. Redner, Phys. Rev. B **36**, 5631 (1987).
 - [10] B. Fourcade and A.-M. S. Tremblay, Phys. Rev. A **36**, 2352 (1987).
 - [11] Y. Meir and A. Aharony, Phys. Rev. A **37**, 596 (1988).
 - [12] T. Nagatani, J. Phys. A **20**, L417 (1987).
 - [13] T. Nagatani, M. Ohki, and M. Hori, J. Phys. A **22**, 1111 (1988).
 - [14] B. B. Mandelbrot, J. Fluid Mech. **62**, 331 (1974).
 - [15] See, e.g., J. Lee *et al.*, Phys. Rev. A **39**, 6545 (1989).
 - [16] P.Ch. Ivanov *et al.*, Nature (London) **399**, 461 (1999).
 - [17] G. Batrouni, A. Hansen, and S. Roux, Phys. Rev. A **38**, 3820 (1988).
 - [18] A. Aharony, R. Blumenfeld, and A. B. Harris, Phys. Rev. B **47**, 5756 (1993).
 - [19] A. Coniglio, J. Phys. A **15**, 3829 (1982).
 - [20] Y. Lee *et al.*, Phys. Rev. E **60**, 3425 (1999).
 - [21] M. Barthélémy *et al.*, Phys. Rev. E **60**, R1123 (1999).
 - [22] In the “two injection points” configuration, the large currents are controlled by the small loops between P and Q . The fluctuation of the length of the shortest path between P and Q gives thus rise to the region of power law behavior for large currents we observe in Fig. 1(b). For the constant current ensemble, the distribution converges to $1/\nu$ for the largest current.